metals

Article

Properties Evaluation of Thin Microhardened Surface Layer of Tool Steel after Wire EDM

Ľuboslav Straka [1,*], Ivan Čorný [2] and Ján Piteľ [3]

[1] Department of Manufacturing Processes Operation, the Technical University of Košice, Štúrova 31, Prešov 08001, Slovakia
[2] Department of Science and Research, the Technical University of Košice, Bayerova 1, Prešov 08001, Slovakia; ivan.corny@tuke.sk
[3] Department of Mathematics, Informatics and Cybernetics, The Technical University of Košice, Bayerova 1, Prešov 08001, Slovakia; jan.pitel@tuke.sk
* Correspondence: luboslav.straka@tuke.sk; Tel.: +421-55-602-6346

Academic Editor: Hugo F. Lopez
Received: 14 March 2016; Accepted: 15 April 2016; Published: 25 April 2016

Abstract: This paper describes results of experimental research on the thin microhardened surface layer of a machined surface that occurs in materials using wire electrical discharge machining (WEDM) with brass wire electrode. The direct influence of microhardened surface layer on resulting machined surface quality of tool steel EN X210Cr12 (W.-Nr. 1.2080) was examined. The aim of the experiment was to contribute to the knowledge of mutual interactions between main WEDM technological parameters, the influence of these parameters on the total affected depth, and on the variation of microhardness of sub-surface layers of machined surface. Based on the microhardness experimental measurements, mathematical models were established by the Least Square Method (LSM) in order to simulate and predict final quality of machined surface after WEDM. Recommendations are given for setting the main technological parameters of the discharge process concerning minimization of total microhardened surface layer depth and microhardened surface layer homogeneity along the whole cross-section profile of the machined surface.

Keywords: machining; heat affected; tool steel; hardness

1. Introduction

In general, achievable qualitative parameters of eroded surface are comparable to the parameters achieved by finishing machining technologies [1,2] such as grinding, honing, lapping, superfinishing, *etc.* However, a complex evaluation of machined surface quality after WEDM is a demanding procedure. To maintain evaluation objectivity, it is necessary to take into account the specifics of this progressive technology [3]. Quality judgments based only on selected parameters—most often these are roughness parameters Ra, Rz, and Ry—can lead to subjective evaluation or even mistakes [4]. In many cases, the character and surface quality, from the aspect of heat treatment, have considerably greater impact on machined surface quality than the roughness itself [5]. Durability and functionality of the surface primarily pre-define its suitable heat treatment or thermo-mechanical treatment. [6] In this sense, significant quality indicators are parameters that characterize the heat-affected zone—its total depth [7], structure [8,9], homogeneity, hardness variation, and hardness course [10].

Considering that electrical discharge machining belongs to thermal processes where certain structural changes may be expected directly under the machined surfaces, as shown by Cusanelli, Hargrove, and Liu [11–13], the total depth of heat affected zone (HAZ) is a very important qualitative parameter. Heat impact on the machined surface is in many cases is an undesirable attendant phenomenon that occurs not only in Wire Electrical Discharge Machining (WEDM) but also in other progressive technologies such as Laser Beam Machining (LBM), Plasma Arc Machining (PAM), *etc*. The overall depth of HAZ and its character are in general closely related to durability and working life of products. This was proven by the research of Švecová [14], Valentinčič [15], and Čada [16]. These authors showed that shearing tools are especially susceptible to undesirable HAZ impact, which causes a decreased working life of the tools. This unwanted effect is caused by the so-called white layer, which presents as a structure occurring after secondary hardening as a consequence of electrical discharge process. However, this should be stated cautiously because certain analyses of Sidhom and Ramesh [17,18] show on the contrary a positive effect of white layer properties. It must be stated though, that this positive effect on operation and surface functionality would manifest itself only in a certain phase of the working life of a machine part. It can be assumed then, that the mastering of the phenomenon with consequent control would make it possible to create surface layers with pre-defined quality. In other cases, as presented by Ho, Newman, Puri, and Bhattacharyya [19,20], the white layer is considered an undesirable phenomenon that indicates high intensity heating during the electrical discharge process. Rapid cooling that follows the electrical discharge process, in combination with extreme or critical setting of the electrical discharge process technological parameters, can even lead to micro-cracks and a burn-eroded surface. This was also confirmed by the research of Deranging, Gangopadhyay, and Biswas [21]. Kiyak and Mathew [22,23] mention that hardenable steels are especially susceptible to micro-cracks—including sample material EN X210Cr12 (W.-Nr. 1.2080). This is due to the fact that, in these steels, there is always a certain amount of retained austenite, which is plastic. Choudhary *et al.* [24] explain this by concentrating on dislocations mostly in austenitic phase during WEDM, which constitutes favorable conditions for micro-cracks creation.

Despite the fact that presently there is a growing emphasis on knowledge complexity of the set of particular characteristics of machined surface after WEDM, a complex identification of interactions between technological processes and material transformations in sub-surface layer, which occur during plastic deformation and heat impact, has not been fully elaborated. The aim of this research was to contribute to the knowledge database of these processes that take place directly on the surface and in the sub-surface layer of a machined surface, and to describe particular relations using mathematical models. Mathematical models are focused on broadening the knowledge concerning HAZ assessment in sub-surface layers of steel EN X210Cr12 machined surface when electrical discharge cutting with a brass wire electrode. Because uncontrolled heat impact has in most cases unwanted, and rarely even fatal consequences, the gained knowledge will have direct application for prediction of machined surface quality after WEDM. Complex management of total HAZ depth and HAZ homogeneity will lead to an increased working life of machine parts and cutting tools such as molds, shearing tools, *etc.* that are made from steel EN X210Cr12 by this progressive electrical discharge technology.

2. Materials and Methods

Experiments were carried out on samples from tool steel EN X210Cr12 (W.-Nr. 1.2080) with bending strength R_{mo} = 3800 MPa and compression yield point R_{et} = 2900 MPa, at basic material hardness 62 HRC (Rockwell Hardness). The material is highly-alloyed chromium ledeburite tool steel with alloying elements contents of 1.80% to 2.05% C and 11.0% to 12.5% Cr. This is used mostly for production of die casting molds and for production of shearing tools for cold shearing. Table 1 shows chemical composition of the steel.

Table 1. Chemical composition of tool steel EN X210Cr12 (W.-Nr. 1.2080).

Designation of Steel	Chemical Composition in (%)							Hardness	
	C	Mn	Si	Cr	Ni	P_{max}	S_{max}	Annealed HB_{max}	Heat-Treated HRC_{min}
EN X210Cr12 (W.-Nr. 1.2080)	1.80–2.05	0.20–0.45	0.02–0.45	11.0–12.5	0.5	0.03	0.035	250	61

The samples were produced on the electrical discharge machine AGIECUT 270HSS (AGIE SA, Losone, Switzerland) shown on Figure 1. It is a Computer numerical control (CNC) device capable of autonomous operation.

Figure 1. CNC electrical discharge machine AGIECUT 270HSS.

Table 2 presents basic technical parameters of CNC electrical discharge machine AGIECUT 270HSS machine.

Table 2. Basic parameters of AGIECUT 270HSS.

Technical Parameter	Maximum Range
portal dimensions X/Y/Z	400/250/251 mm
workpiece dimensions X/Y/Z	1050/650/250 mm
workpiece weight	400 kg
inclination angle	30/100 mm
wire diameter	0.1–0.3 mm
shape tolerance	±3 µm

The cutting tool used in the experiment was brass Ms63 wire electrode of 0.25 mm diameter. Material Ms63 is a compound $CuZn_3$ that contains 63% Cu and 37% Zn [25]. Working fluid was non-ionized water with electric conductivity no more than 150 $\mu s \cdot cm^{-1}$.

The basic technological parameters of WEDM that influence final quality of machined surface with regard to the total HAZ depth in essential way include: peak current I (A), pulse on-time duration t_{on} (µs), and consequent break for renewal of discharge channel called pulse off-time duration t_{off} (µs), and voltage of discharge U (V). Expected influence of primary technological parameters of electrical discharge process on quality of machined surface of steel EN X210Cr12 after WEDM with brass 0.25-mm diameter Ms63 wire electrode in terms of the total HAZ depth and the parameters setting ranges applied in the experiment are shown in Table 3.

Table 3. Setting ranges of main WEDM technological parameters applied in experiment at machining of steel EN X210Cr12 with Ms63 electrode, and their expected influence on microhardness variation.

Main Technological Parameters	Type of Operation	Setting Range	Influence of Technological Parameter on HAZ
Maximum peak current I (A)	roughing finishing	10.5–15.0 1.0–4.5	With increase of I value, total HAZ depth grows markedly
Pulse on-time duration t_{on} (µs)	roughing finishing	11.5–16.0 2.5–7.0	With increase of t_{on} value, total HAZ depth grows markedly
Pulse off-time duration t_{off} (µs)	roughing finishing	4.5–8.5 6.5–10.0	With increase of t_{off} value, total HAZ depth reduces slightly
Voltage of discharge U(V)	roughing finishing	85–90 65–70	With increase of U value, total HAZ depth grows slightly

2.1. The Basic Characteristic of Eroded Surface and HAZ after WEDM

As mentioned in the Introduction, the eroded surface of the material after WEDM is matte; however, its roughness parameters are comparable to ground surfaces. Relatively high surface quality steel EN X210Cr12 samples, according to roughness parameters in the ranges of Ra = 0.8 to 3.7 μm, Ry = 5.8 to 25.4 μm, and Rz = 5.1 to 22.8 μm, was recorded by surface roughness tester Mitutoyo Surftest SJ-400 (Mitutoyo Corporation, Kawasaki, Japan). The quality of the surface was achieved by applying suitable combination of technological parameters of electrical discharge process during the experiment. Higher values of roughness Ra, Ry, and Rz were achieved at roughing operations, while lower values correspond to finishing operations. It can be observed on the eroded surface of the steel EN X210Cr12 samples that due to the discharge plasma channel with high density and intensity (and simultaneous high temperature impact), structural changes appear on the surface layers of basic material [26], while integrity of the material was preserved. Micro-cracks or other disintegrations were not observed on the surface or in the sub-surface layer. This is attributed to proper preparation of the samples using heat treatment [27] in combination with favorable electric and heat conductivities ($G = 1.54\ \mathrm{S \cdot m^{-1} \cdot mm^{-2}}$; $\lambda_t = 30\ \mathrm{W \cdot m^{-1} \cdot K^{-1}}$) of the applied steel EN X210Cr12. Figure 2 shows allocation of particular sub-surface layers of untreated eroded sample surface observed by the digital microscope Keyence VK-X150 (Keyence International, Mechelen, Belgium) at 1000× magnification where structural changes occur in the terms that represent technological parameters setting for roughing operations.

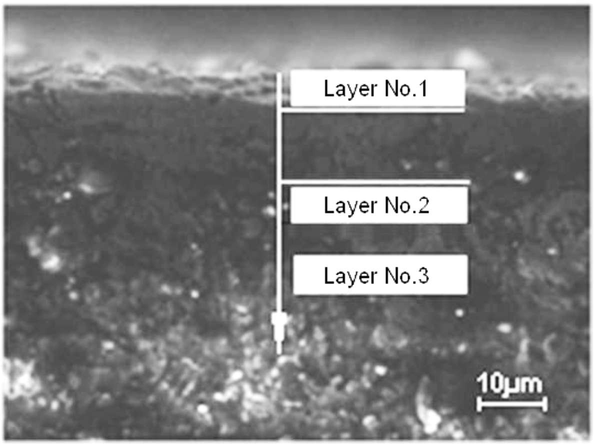

Figure 2. Allocation of particular sub-surface layers of experimental sample made by electrical discharge technology in the terms that represent technological parameters setting for roughing operation (1000× magnification).

Layer No. 1 is characterized by burn-erosion and is created by metal remnants from the tool—brass Ms63 wire electrode. Layer No. 2 represents the heat-affected zone that consists of white layer and transition layer. The border between these two layers is visible as shown in Figure 2 at 1000× magnification, where strong microstructure change is present. Layer No. 3 represents basic material with no heat impact and structural variations due to the electrical discharge process. The border between layer No. 2 and layer No. 3 cannot be identified as a clear line because the structure of layer No. 2 gradually merges into layer No. 3. The exact border could only be determined on the basis of microhardness variation (measured according Vickers Hardness Test method described in Section 2.3).

2.2. Preparation of Experimental Samples

The samples for the experiment were made from steel blocks with dimensions 100 × 150 × 50 mm from material EN X210Cr12. Before eroding, the sample material was quench-hardened to a hardness of approximately 64 HRC [28]. It was hardened in oil at a temperature of 950 °C (Figure 3) with consecutive tempering (Figure 4) to hardness approximately 61 HRC at a temperature of 220 °C in order to remove internal stresses that emerged during hardening.

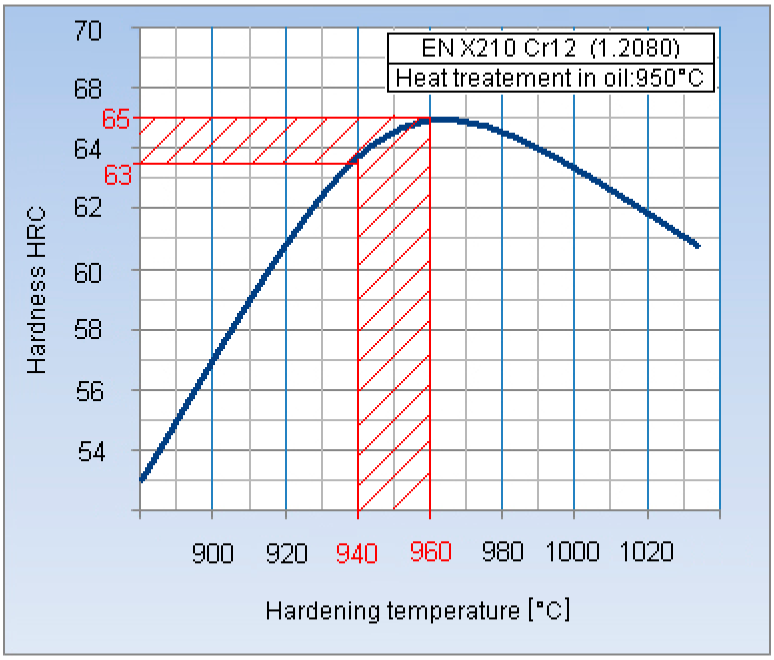

Figure 3. Hardening diagram of steel EN X210Cr12 [29].

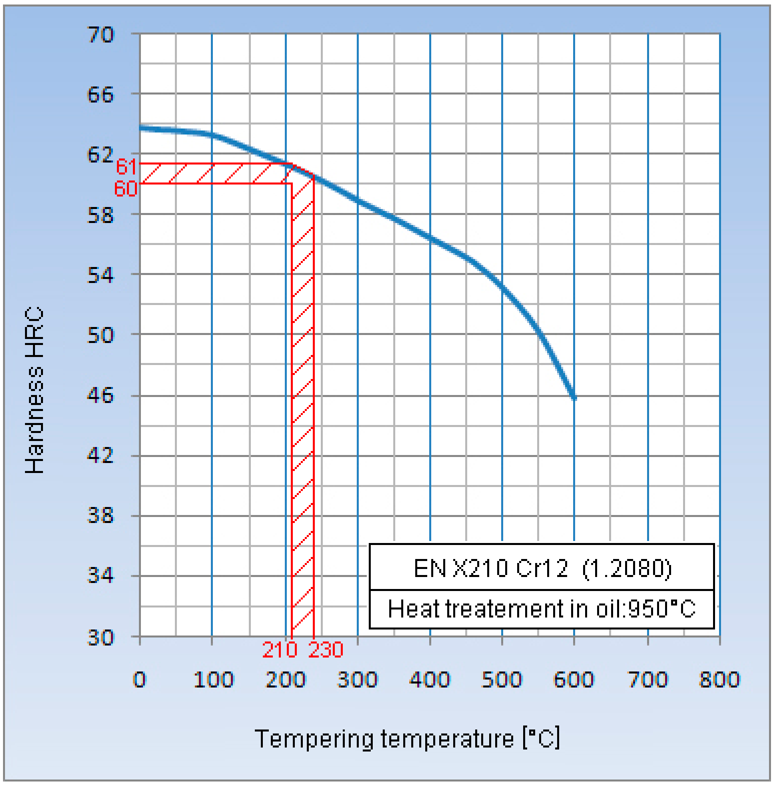

Figure 4. Tempering diagram of steel EN X210Cr12 [29].

On the eroded surface layer of the samples, a mild burn-erosion could be clearly observed (black stains on the surface) without visible micro-cracks or macro-cracks (Figure 5). At the same time, a slight oxidative layer (rust) was present on the surface (visually observed as an orange coating).

Figure 5. Burn-eroded surface of the sample made from steel EN X210Cr12 after WEDM.

Picture of the eroded surface of the steel EN X210Cr12 sample recorded using the scanning digital microscope Keyence VK-X150 at 500× magnification shows small metal particles (whitish stains). These particles were melted out from the Ms63 electrode (Figure 6). In order to avoid distortion of experimental results due to disturbances caused by the particles, it was necessary to adjust the eroded surfaces before measurements.

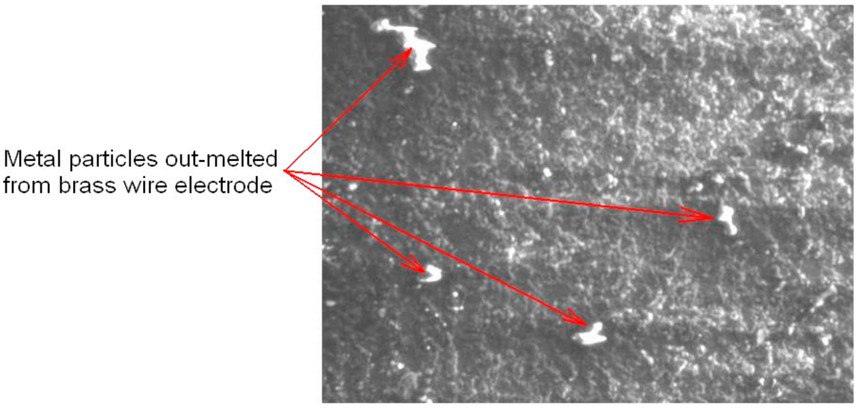

Figure 6. Eroded surface layer of the steel EN X210Cr12 after WEDM (500× magnification).

Whereas the electrical discharge process was carried out in the presence of dielectric liquids on the basis of non-ionized water, which to some extent has a corrosive effect on the material EN X210Cr12, it was necessary to remove subtle oxidative layer (aqueous corrosion) from the eroded surface of the samples. The oxidative layer was removed from the surface by acid pickling with a solution based on phosphoric acid (H_3PO_4 of 90% concentration), and by pickling agent Armohib 25 at a constant temperature of 20 °C and a 5-min actuation time. To ensure correct measurements of surface hardness, it was also necessary to remove fine brass particles from the surface; these are the remnants of the wire electrode. The brass particles were removed from the eroded surface using chemicals. The surface was rinsed with a solution of water and concentrated ammonia (0.9 g$\cdot$cm^{-3}) with ratio 9 to 1 (water to ammonia) plus additives: ammonium persulfate (0.2 g per 10 cm^{-3} of solution) and sodium phosphate (0.1 g per 10 cm^{3} of solution). Then, the etched-out metal remnants were removed from the surface by blasting with glass spheres of 50 μm diameters, and a spot load of blasting spheres for approximately

3 s on cm^2 of the surface from 40 mm distance at 30° angle. The samples were then ready for evaluation of the HAZ parameters.

2.3. Microhardness Test and Measurement of Total HAZ Depth

To determine suitable measuring procedures for HAZ depth, it was inevitable to consider the specifications of the given progressive technology where heat impact and consequent microhardness variations occur instantly after high temperature electrical discharge channel spot impact. The electrical discharge originates between the wire electrode as a cutting tool and the metal material as a workpiece with simultaneous intensive cooling by dielectric liquid. The heat affected zone shows different values in straight direction and in cross-section direction concerning wire electrode movement against the workpiece. Similarly, the course of HAZ time depends on combination of settings of main technological parameters. It is necessary to set the technological parameters with regard to the electrical discharge cutting process itself, as well as electrochemical properties of the material.

The achieved total HAZ depth and variation of microhardness is closely coupled with properties of the applied material EN X210Cr12, and setting values of main technological and process parameters [30,31]. According to papers by several authors mentioned in the Introduction, it can generally be assumed that the strongest impact of these parameters will manifest at power/roughing operations, while the least impact will be observed at fine finishing operation. Values of total HAZ depth and course of microhardness were examined by measurements in sub-surface layers. To evaluate the total HAZ depth, it was very important to take into account possible scattering of microhardness values with consideration of the structure of applied material. Because microhardness course will not likely be the same along the whole cross-section, it was decided to carry out measurements in several parallel lines.

Considering the supposedly very small total depth of the heat-affected zone, the value of which fall into tens of micrometers, it was essential to establish a proper method for microhardness measurement. The suitable application method appeared to be the method of beveled cross-section, which best respects specifics of the given technology. For exact evaluation of microhardness of sub-surface layers of the samples, it was necessary to prepare metallographic specimens at very low angles due to supposed maximum HAZ depth of 60 μm produced by roughing operation.

The microhardness measurements were carried out on metallographic specimen of samples from steel EN X210Cr12 (Figure 7) prepared at angle $\alpha = 0.03$. Total length of metallographic specimen lv at supposed total HAZ depth $h_{\mathrm{HAZt}} = 60$ μm was calculated by the formula:

$$lv = \frac{h_{\mathrm{HAZt}}}{\sin\alpha} = 115\ \mathrm{mm} \quad (1)$$

where lv is total length of metallographic specimen, h_{HAZt} is theoretical (supposed) total HAZ depth, and α is angle of metallographic specimen.

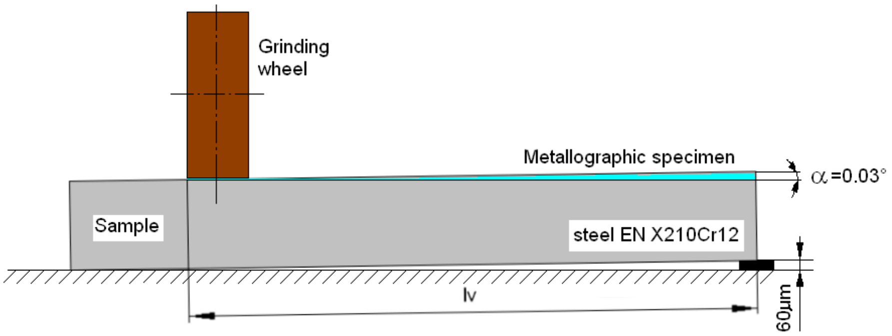

Figure 7. Procedure of preparation of metallographic specimen with beveled cross-section method on experimental sample from steel EN X210Cr12 at 0.03° angle.

Hardness of basic material of evaluated samples ranges from 60 to 62 HRC, so the Vickers microhardness test, according to norm EN ISO 6507 [32], could not be applied. The load in this test ranges from 0.098 to 0.98 N, which is not enough for basic material hardness 60 to 62 HRC. At this load, it is possible to measure microhardness to maximum value 464 HV0.1, which corresponds to a Rockwell hardness of approximately 46 HRC. Therefore, Vickers hardness test at low load HV2 was applied. According to the norm, the prescribed load of indenter is 19.61 N.

Hardness measurements on metallographic specimens in heat affected zone of the experimental samples of 50 mm thickness was carried out on Zwick ZHV30 Vickers Hardness Tester (Zwick GmbH&Co, Ulm, Germany) with measuring range HV0.2 to HV30.

3. Results and Discussions

3.1. Experimental Measurement of Total HAZ Depth and Microhardness Course

The total HAZ depth measurements consisted of indentations carried out in a line from the specimen edge to the material core in 5 mm distances (Figure 8). The measurement was finished when three consequent microhardness values have settled on constant value, *i.e.*, a hardness value of the basic material that is approximately 740 HV. Every indentation represented an increment 2.62 μm of total HAZ depth.

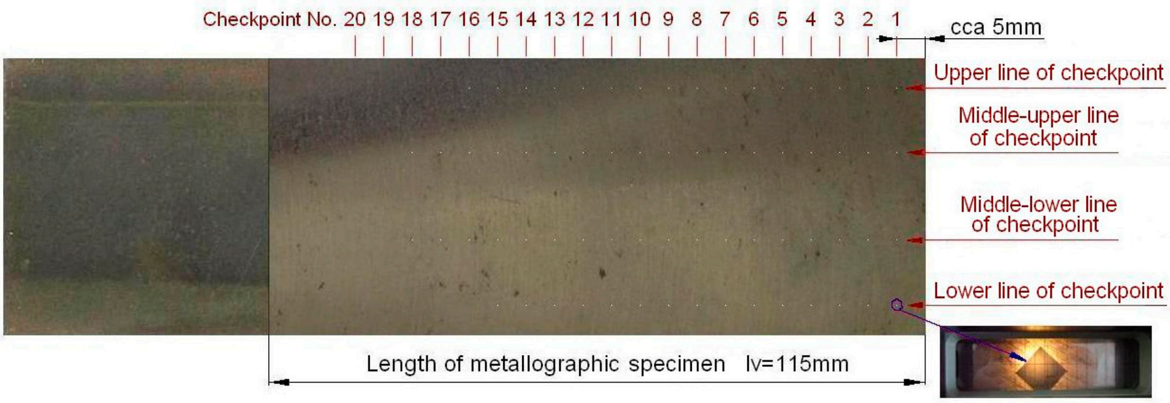

Figure 8. Testing of total HAZ depth on metallographic specimen of the sample made from steel EN X210Cr12 with Zwick ZHV30 Vickers Hardness Tester.

In order to respect the profile character, surface micro-geometry, and microhardness course in the axis of the cut, the indentations were carried out in four parallel lines, *i.e.*, in two marginal and two central lines in the same distance of the specimen edge. Marginal lines were located 5 mm from the specimen edge, while central lines were located at approximately 1/3 of the material thickness.

3.2. Evaluation of Experimental Measurements

Figure 9 shows metallographic snapshot recorded by scanning electron microscope JEOL 5900 LV (JEOL Ltd., Tokyo, Japan). The picture depicts HAZ on one of the experimental specimens from steel EN X210Cr12 together with microhardness course in particular sub-surface layers.

Figures 10 and 11 show courses of HV2 microhardness created from measured values of microhardness in particular layers of HAZ samples from steel EN X210Cr12. The samples were made by application of roughing and finishing operations, respectively.

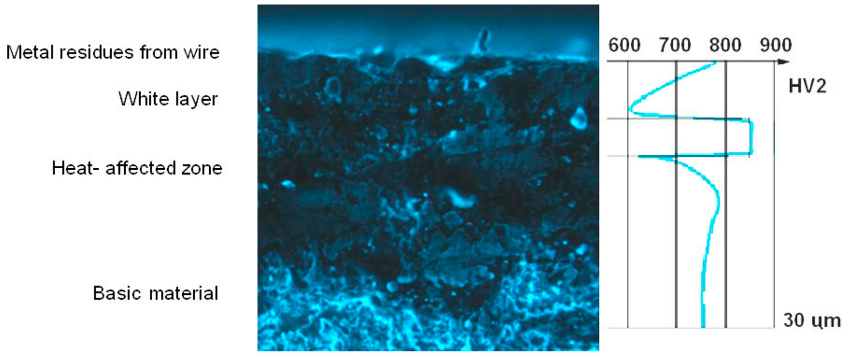

Figure 9. Microhardness variation in the particular heat affected sub-surface layers of the sample made using WEDM from steel EN X210Cr12 is graphically represented by the curve (blue line); and metallographic image recorded by electron microscope JEOL 5900 LV (1000× magnification).

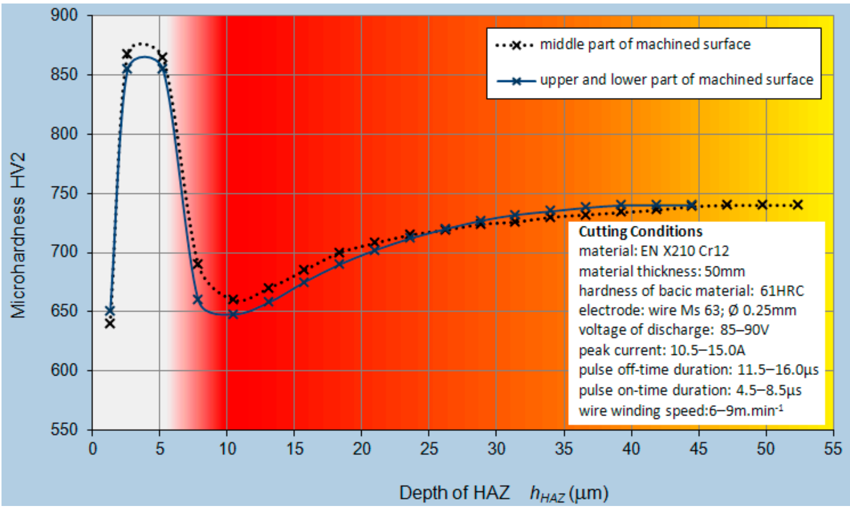

Figure 10. Course of HV2 microhardness in the particular heat affected sub-surface layers of the samples from steel EN X210Cr12 made by WEDM roughing.

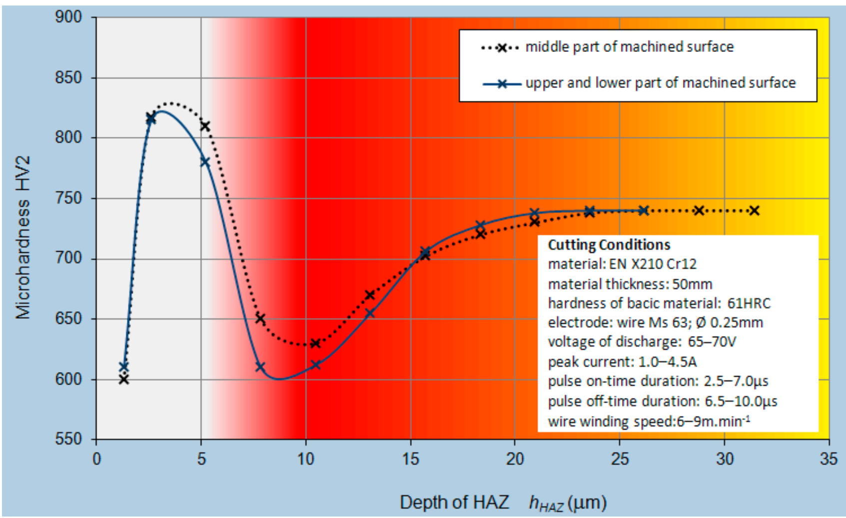

Figure 11. Course of HV2 microhardness in the particular heat affected sub-surface layers of the samples from steel EN X210Cr12 made by WEDM finishing.

The graphs in Figures 10 and 11 present essential variations of microhardness directly on the surface as well as in adjacent sub-surface eroded layers of steel EN X210Cr12 in comparison to the hardness of original material 740 HV2. In compliance with the assertion of Che Haron *et al.* and m it was proven that hardness on eroded surface is significantly decreased compared to the basic material hardness; its value ranging from 600 to 650 HV2. This holds true for power/roughing as well as finishing machining. The method of machining has almost negligible influence on the microhardness variations in this layer. Certain slight differences were observed between central and marginal lines of the eroded surface. On the contrary, essential influence of machining method on microhardness variations was observed in the zone of "white layer", where microhardness grows substantially from 820 to 870 HV2, then drops again to the range of 610 to 660 HV2. Lower values were achieved at finishing operations, and higher values at roughing operations. In the transition zone, significant differences in gradual microhardness increase can also be observed. Microhardness values of basic material were achieved using both methods of machining in a depth range of approximately 20 to 50 µm. At the same time, it was observed that the total recorded HAZ depth significantly depends on machining method. Markedly lower values of HAZ total depth were recorded using finishing operations, where total HAZ depth spanned from 20 to 25 µm, while higher values ranging from 40 to 50 µm were achieved using roughing operations. Courses of microhardness at finishing operations followed steeper curves than those at roughing operations.

Figures 12 and 13 show measured values of thicknesses of particular sub-surface layers of HAZ in various parts of the eroded surface of samples made from steel EN X210Cr12 at roughing/power operations and finishing operations.

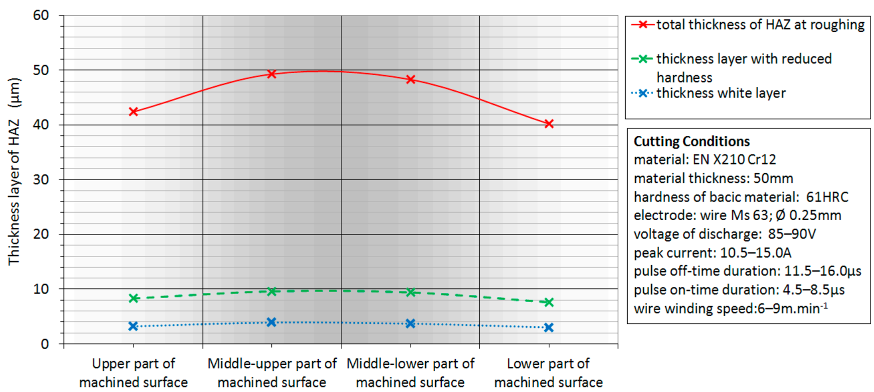

Figure 12. Total thicknesses of two basic HAZ layers in the particular parts of eroded surface of the sample from steel EN X210Cr12 at roughing operations.

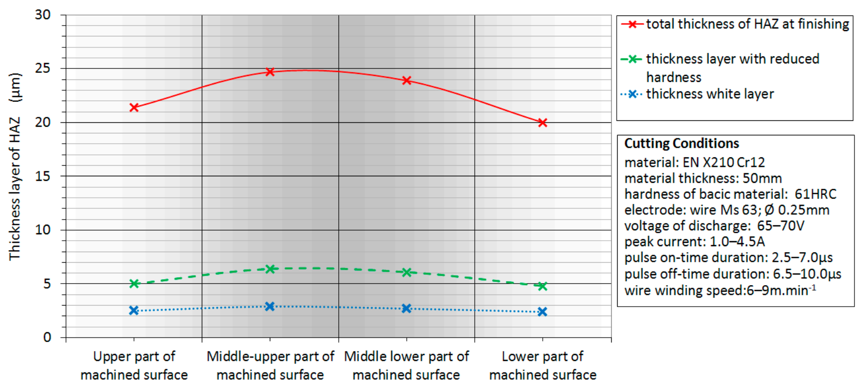

Figure 13. Total thicknesses of two basic HAZ layers in the particular parts of eroded surface of the sample from steel EN X210Cr12 at finishing operations.

It is evident from the graphs shown in Figures 12 and 13 that the total thicknesses of particular layers of HAZ of the eroded surface of the samples depend significantly on machining method, *i.e.*, whether it is roughing or finishing operations, with higher values recorded for roughing and lower values for finishing operations. Thickness of white layer spanned in this case in range from 3 to 6 μm; thickness of transitional layer spanned from 15 to 40 μm. At the same time, the differences of microhardness between central and marginal line of eroded surface were observed. In the central part, total HAZ depth reached values 20% higher than at the margins. These differences were likely caused by heating of the material to higher temperature, and due to lower cooling intensity by dielectric liquid. This effect was not as sharp at finishing operations where the intensity of discharge channel was lower, and at the same time better circulation of dielectric liquid was assured. In this way, a higher efficiency of cooling of basic material was achieved compared to power/roughing cuts.

3.3. Mathematical Modeling of the Total HAZ Course

To be able to predict surface quality concerning total HAZ depth, it was necessary to establish mathematical models [35–37] that would represent behavior of machined surface, depending on the main technological parameters [38]. Therefore, the primary task of the experiment was to establish mathematical models, in particular cross-sections, on the basis of measured values of real microhardness course, and total HAZ depth course. The models would enable simulation of final quality of surface after WEDM, including recommendations for the settings of main technological parameters of electrical discharge process with regard to minimization of total HAZ depth, and best HAZ homogeneity along the cut profile.

Least Squares Method (LSM) appears to be suitable method for modeling of total HAZ depth after WEDM. It approximates n-tuple measured values $[x_1,x_2, \ldots x_m,y]$ by function of m variables in the form:

$$y = f(x_1, \ldots, x_m) \tag{2}$$

where y represents functional dependence of total HAZ depth, and $x_1, \ldots, x_m$ are real measured values of total HAZ depth.

According to character and distribution of measured values, an exponential function was considered with the base of any natural number in the form:

$$y = a_{00} \cdot a_{10}^{x_1} \cdot a_{01}^{x_2} \cdot a_{11}^{x_1 x_2} \tag{3}$$

where x_1, x_2 represents main technological parameters, and $a_{00}, \ldots, a_{11}$ are unknown variables.

While an important condition was that function $S(A)$, expressing the sum of squares of differences of the calculated and measured values in all cases, has reached the minimum according to the relationship:

$$S(A) = \sum_{i=1}^{r} \left[y_i - f(x_1, ..., x_m, A)\right]^2 \tag{4}$$

Consecutively, particular values $f(x_1, ..., x_m, A)$ were substituted by chosen function. Since the function has several variables, namely unknown matrix A, on the basis of the necessary condition specific for the existence of extreme of such a function, first partial derivatives of $S(A)$ must be equal to zero. Then, we obtain relationships to calculate the unknown coefficients:

$$\frac{\partial S(a_{00}, \ldots, a_{rr})}{\partial a_{ij}} = 0 \text{ for } i,\ j = 0,\ \ldots,\ r \tag{5}$$

From the adjusted partial derivatives, we obtain a system of linear equations; the solutions of which are the sought coefficients.

The quality of the approximation of experimentally measured values of the individual parameters, provided that the regression model describes the course, is expressed by the correlation index *IK*, which can be calculated by the formula:

$$IK = \sqrt{1 - \frac{\sum_{i=1}^{n} (y'_i - y_i)^2}{\sum_{i=1}^{n} (\overline{y_i} - y_i)^2}} \tag{6}$$

where y'_i represents calculated values of h_{HAZ} according to the established function for $I = 1, \ldots, n$, y_i are measured h_{HAZ} values, and $\overline{y_i}$ is arithmetic average of measured values h_{HAZ}.

Because the total depth of the HAZ is affected essentially by discharge peak current *I*, and pulse on-time duration t_{on}, the mathematical model was established on an approximation of the measured values of these two technological parameters, and total depth of heat affected zone h_{HAZ}, as a function of seven variables in the form:

$$h_{\mathrm{HAZ}} = a_{00} \cdot a_{10}{}^{I} \cdot a_{20}{}^{I^2} \cdot a_{30}{}^{I^3} \cdot a_{01}{}^{t_{on}} \cdot a_{02}{}^{t_{on}{}^2} \cdot a_{03}{}^{t_{on}{}^3} \tag{7}$$

which approximates n-tuple measured values $\left[I_i, t_{\mathrm{on}i}, h_{\mathrm{HAZ_i}}\right]$ with function:

$$h_{\mathrm{HAZ}} = f(I,\, t_{\mathrm{on}}, \boldsymbol{A}) = f(I,\, t_{\mathrm{on}}, a_{00}, \ldots a_{\mathrm{rr}}) \tag{8}$$

where the unknown parameters a_{ij}, $i, j = 0,\ldots,r$ are calculated in such a way that the area *S(A)* would best approximate the functional values measured. In that case, we can adjust Equation (4) into shape

$$S(A) = \sum_{i=1}^{n} \left[h_{\mathrm{HAZ}i} - f\left(I_i, t_{\mathrm{on}i}, A\right)\right]^2 \tag{9}$$

provided the given function reaches a minimum. In this case, the matrix of variables a_{ij} is unknown parameter.

On the basis of the measured values of the total depth of the heat affected zone h_{HAZ} of steel EN X210Cr12 at various maximum peak current *I* and various on-time pulse duration t_{on}, and applying MS Office EXCEL using an approximation logarithmic function LOGEST, the mathematical model was established. The result of the mathematical model is an array of values that describe the area.

Mathematical model of total HAZ depth valid for roughing/power operations:

$$h_{\mathrm{HAZ}} = 1.47 \cdot 10^{-9} \cdot 0.6099^{I} \cdot 1.0489^{I^2} \cdot 0.9986^{I^3} \cdot 159.4418^{t_{\mathrm{on}}} \cdot 0.7138^{t_{\mathrm{on}}{}^2} \cdot 1.0075^{t_{\mathrm{on}}{}^3}\ (\mu\mathrm{m}) \tag{10}$$

Correlation index is $IK^2 = 0.9980$.

Mathematical model of total HAZ depth valid for finishing operations:

$$h_{\mathrm{HAZ}} = 5.0007 \cdot 1.3857^{I} \cdot 0.9115^{I^2} \cdot 1.0095^{I^3} \cdot 1.6308^{t_{\mathrm{on}}} \cdot 0.9374^{t_{\mathrm{on}}{}^2} \cdot 1.0028^{t_{\mathrm{on}}{}^3}\ (\mu\mathrm{m}) \tag{11}$$

Correlation index is $IK^2 = 0.9969$.

where h_{HAZ} is total HAZ depth (μm), *I* is discharge peak current (A), and t_{on} is pulse on-time duration (μs).

Established mathematical models have been implemented in the Graphics simulation program to create 3D graphical dependencies (Figures 14 and 15) of total HAZ depth of steel EN X210Cr12 with a thickness 50 mm on two significant technological parameters, WEDM roughing and WEDM finishing.

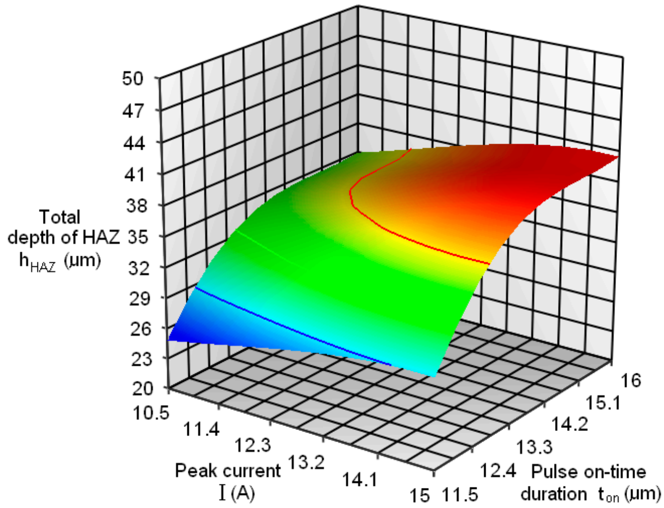

Figure 14. 3D simulation of dependence of total HAZ depth of steel EN X210Cr12 samples after WEDM roughing.

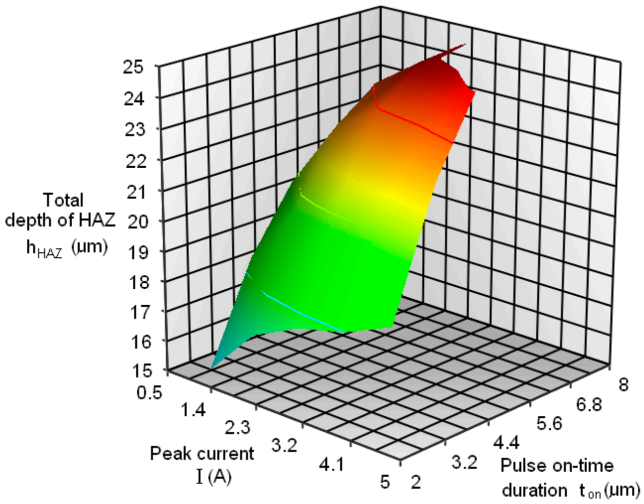

Figure 15. 3D simulation of dependence of total HAZ depth of steel EN X210Cr12 samples after WEDM finishing.

Experimentally established mathematical models describe in detail the dependence of the total HAZ depth on settings of two important technological WEDM parameters, *i.e.*, discharge peak current I and pulse on-time duration t_{on}. The models provide a tool for the simulation of optimal settings of the parameters. Precision of established mathematical models for the total HAZ depth is indicated by the correlation index. This index is 0.9980 for roughing, *i.e.*, power operations. For finishing operations, the index reaches value 0.9969, which means the deviations of calculated values from real values are in the range of 0.3%.

On the basis of presented 3D simulation of total HAZ depth dependence on two significant technological parameters of WEDM of steel EN X210Cr12, the optimal setting values of main technological parameters (for both roughing and finishing operations) are located in area outlined by blue and red line (green area in Figures 14 and 15).

On the basis of a detailed investigation of the total depth of HAZ, and microhardness variations in sub-surface layers of the eroded surface, relying on the mathematical models, it can be stated that the high setting of both technological parameters, *i.e.*, peak current I, and pulse on-time duration t_{on}, or their unsuitable combination, resulted in a substantial increase of total HAZ depth, and a negative impact on variations and course of the microhardness in HAZ. However, by optimizing of the setting of the main technological parameters, surfaces can be created with the required value of h_{HAZ} parameter, as well as the required value and level of homogeneity of microhardness. It must be noted, though, that in setting of main technological parameters, it is also necessary to take into account the performance and productivity of the cutting process. This means that the actual setting values of the main technological parameters of WEDM must, in addition to maximizing the machined surface quality indicators, also be optimized both in terms of maintaining the stability and performance of the cutting process with a regard to achieving the greatest cutting power. Therefore, an appropriate solution may be, for example, setting a higher value for the t_{off} of about 20%, which will lead to a minimal reduction of the cutting performance due to the share of idle running, however it will also lead to a substantial homogenization of particular values of observed parameters h_{HAZ} and microhardness between the central and marginal lines of the eroded surface. Changing this technological parameter will increase the time needed to cool the sub-surface layers of machined material, leading to a reduction of an impact range, and at the same time to an increase of the homogeneity of the quality parameters of the heat-affected zone throughout the profile of machined surface after WEDM. An increase of the pulse off-time duration t_{off} higher than 20% and related change of the idle running can cause quite the opposite phenomenon, which in turn will lead to higher influence on marginal lines of the eroded surface.

4. Conclusions

The objectives of the experiment were to carry out detailed research of the thin microhardened surface layer of machined surface at wire electrical discharge cutting of steel EN X210Cr12 (W.-Nr.1.2080) with brass Ms63 wire electrode of 0.25 mm diameter; to evaluate consequences of HAZ on final quality of machined surface; and to contribute to the knowledge database of HAZ at electrical discharge process. Within the experiment, the detailed evaluation of thin surface layer of the eroded surface was carried out in terms of overall thickness, range and microhardness variation. To achieve required surface quality of machined surface in terms of h_{HAZ}, it was necessary to establish mathematical models that would describe behavior of machined surface in relation to the settings of main technological parameters with regard to the real microhardness course. Mathematical models were implemented into a simulation program, which enabled specifying an optimal combination of main technological parameters with focus on the required value of the h_{HAZ} parameter.

The results of the experiment can be summed up in the following points:

(i) Total microhardened surface layer depth determined by experimental measurement on tool steel EN X210Cr12 ranges from 20 to 25 μm for finishing operations and from 40 to 50 μm for roughing operations.

(ii) Differences of measured values of total microhardened surface layer depth were found in particular lines of the cut; marginal parts of eroded surface at 50 mm thickness of the material showed approximately 20% lower values of h_{HAZ} than middle part.

(iii) In the heat affected zone, an essential fluctuation of microhardness was observed considering hardness of basic material, which was on the level approximately 740 HV2; microhardness in the so-called "white layer" zone showed increased values ranging from 870 to 820 HV2. On the contrary, in the transition layer, a microhardness decrease was recorded to the level of 610 to 660 HV2.

(iv) The knowledge gained by the experimental research of heat affected zone of machined surface of tool steel EN X210Cr12 after WEDM concerning microhardness variation and total HAZ depth presents an important contribution, not only on a theoretical level, but also for manufacturing practice: the results of the research will enable meeting tighter quality requirements on machined surface after WEDM and, thus, to achieve higher quality of products in the same time, decreasing the scrap factor.

Acknowledgments: This research work was supported by the Project of the Structural Funds of the EU, ITMScode 26220220103.

Author Contributions: L'uboslav Straka conceived and designed the experiments; L'uboslav Straka and Ivan Čorný performed the experiments; L'uboslav Straka and Ján Piteľ analyzed the data; L'uboslav Straka wrote the paper.

Conflicts of Interest: The authors declare no conflict of interests.

Abbreviations

The following abbreviations are used in this manuscript:

WEDM	Wire Electrical Discharge Machining
CNC	Computer numerical control
HAZ	Heat Affected Zone
HV2	Vickers Hardness
HRC	Rockwell Hardness
LSM	Least Square Method
LBM	Beam Machining
PAM	Plasma Arc Machining

References

1. Kopac, J. High precision machining on high speed machines. *J. Achiev. Mater. Manuf. Eng.* **2007**, *24*, 405–412.
2. Zhang, J.; Li, Q.; Zhang, H.; Sui, Y.; Yang, H. Investigation of micro square structure fabrication by applying textured cutting tool in WEDM. *Micromachines* **2015**, *6*, 1427–1434. [CrossRef]
3. Maňková, I. *Progressive Technologies*, 1st ed.; SjF TUKE: Kosice, Slovakia, 2000; p. 275.
4. Fernández, P.; Blanco, D.; Rico, C.; Valiño, G.; Mateos, S. Influence of surface position along the working range of conoscopic holography sensors on dimensional verification of AISI 316 wire EDM machined surfaces. *Sensors* **2014**, *14*, 4495–4512. [CrossRef] [PubMed]
5. Zaborowski, T.; Jurko, J.; Panda, A. *Damage-Wear of the Cutting Tool*, 1st ed.; IBEN Gorzow Wlkp.: Poznaň, Poland, 2014; p. 127.
6. Straka, L'.; Čorný, I. Heat treating of chrome tool steel before electroerosion cutting with brass electrode. *Acta Metall. Slovaca* **2009**, *15*, 180–186.
7. Ťavodová, M. Research state heat affected zone of the material after wire EDM. *Acta Fac. Tech.* **2014**, *19*, 145–152.
8. Mičietová, A.; Neslušan, M.; Čilliková, M. Influence of surface geometry and structure after non-conventional methods of parting on the following milling operations. *Manuf. Technol.* **2013**, *13*, 199–204.
9. Zajac, J.; Mitaľ, D.; Radchenko, S.; Jadušová, A.; Straka, R. Study of the subsurface layers of the structural ceramics WC–Co alloyed by laser. In Proceeding of the IEEE 17th International Conference on Intelligent Engineering Systems, San José, Costa Rica, 19–21 June 2013; pp. 307–310.
10. Shrestha, T.; Alsagabi, S.F.; Charit, I.; Potirniche, G.P.; Glazoff, M.V. Effect of heat treatment on microstructure and hardness of grade 91 steel. *Metals* **2015**, *5*, 131–149. [CrossRef]
11. Cusanelli, G.; Hessler-Wyser, A.; Bobard, F.; Demellayer, R.; Perez, R.; Flükiger, R. Microstructure at submicron scale of the white layer produced by EDM technique. *J. Mater. Process. Technol.* **2004**, *1*, 289–295. [CrossRef]
12. Hargrove, S.K.; Ding, D. Determining cutting parameters in wire EDM based on workpiece surface temperature distribution. *Int. J. Adv. Manuf. Technol.* **2007**, *34*, 295–299. [CrossRef]
13. Liu, J.F.; Guo, Y.B. Surface integrity evolution from main cut mode to finish trim cut mode in W-EDM of shape memory alloy. *Appl. Surf. Sci.* **2014**, *308*, 253–260. [CrossRef]
14. Švecová, V.; Madaj, M. Surface characteristics evaluation of the VANADIS 23 high speed steel punch after Wire Electrical Discharge Machining. *Stroj. Technol.* **2012**, 40–41.
15. Valentinčič, J.; Brissaud, D.; Junkar, M. EDM process adaptation system in toolmaking industry. *J. Mater. Process. Technol.* **2005**, *2*, 291–298. [CrossRef]

16. Čada, R.; Zlámalík, J. Materials comparison of cutting tools functional parts for cutting of electrical engineering sheets. *Trans. VŠB–Ostrava Mech. Ser.* **2012**, 33–41.
17. Ramesh, S.; Natarajan, N.; Krishnaraj, V. Effect of multipass cutting on surface roughness in wire electrical discharge machining of metal matrix composites. *Carbon Sci. Technol.* **2014**, *3*, 14–21.
18. Sidhom, H. Effect of electro discharge machining (EDM) on the AISI316L SS white layer microstructure and corrosion resistance. *Int. J. Adv. Manuf. Technol.* **2012**, *1–4*, 141–153. [CrossRef]
19. Ho, K.H.; Newman, S.T. State of the art electrical discharge machining (EDM). *Int. J. Mach. Tools Manuf.* **2003**, *13*, 1287–1300. [CrossRef]
20. Puri, A.B.; Bhattacharyya, B. Modeling and analysis of white layer depth in a wire-cut EDM process through response surface methodology. *Int. J. Adv. Manuf. Technol.* **2005**, *3–4*, 301–307. [CrossRef]
21. Dewangan, S.; Gangopadhyay, S.; Biswas, C.K. Study of surface integrity and dimensional accuracy in EDM using Fuzzy TOPSIS and sensitivity analysis. *Measurement* **2015**, *63*, 364–376. [CrossRef]
22. Kiyak, M.; Cakir, O. Examination of machining parameters on surface roughness in EDM of tool steel. *J. Mater. Process. Technol.* **2007**, *1–3*, 41–144. [CrossRef]
23. Mathew, S.; Varma, P.R.D.; Kurian, P.S. Study on the Influence of process parameters on surface roughness and MRR of AISI 420 stainless steel machined by EDM. *Int. J. Eng. Trends Technol.* **2014**, *2*, 54–58. [CrossRef]
24. Choudhary, R.; Kumar, H.; Gark, R.K. Analysis and evaluation of heat affected zones in electric discharge machining of EN-31 die steel. *Indian J. Eng. Mater. Sci.* **2010**, *2*, 91–98.
25. Ma, A.; Zhu, C.; Chen, J.; Jiang, J.; Song, D.; Ni, S.; He, Q. Grain refinement and high-performance of equal-channel angular pressed Cu–Mg alloy for electrical contact wire. *Metals* **2014**, *4*, 586–596. [CrossRef]
26. Chotěborský, R.; Linda, M.; Ružbarský, J.; Muller, M. Modelling of the anisothermal phase transformation of austenite by electromagnetic sensor. *Appl. Mech. Mater.* **2014**, *616*, 44–51. [CrossRef]
27. Tie, D.; Guan, R.G.; Guo, N.; Zhao, Z.; Su, N.; Li, J.; Zhang, Y. Effects of different heat treatment on microstructure, mechanical and conductive properties of continuous Rheo-extruded Al-0.9Si-0.6Mg (wt %) alloy. *Metals* **2015**, *5*, 648–655. [CrossRef]
28. Orečny, M.; Buršak, M.; Viňaš, J. The influence of heat treatment on the abrasive wear resistance of a construction and a tool steel. *Metalurgija* **2015**, *54*, 91–193.
29. Material Card of Steel EN X210Cr12. Available online: http://www.usbcosteels.com/pdffile/OCR12.pdf (accessed on 18 April 2016).
30. Kim, J.M.; Ha, T.H.; Park, J.S.; Kim, H.G. Effect of laser surface treatment on the corrosion behavior of FeCrAl-coated TZM alloy. *Metals* **2016**, *6*, 29. [CrossRef]
31. Straka, L'.; Hašová, S. Study of tool electrode wear in EDM process. *Key Eng. Mater.* **2016**, *669*, 302–310. [CrossRef]
32. STN ISO 6507 Hardness Measurement. Available online: http://infostore.saiglobal.com/store/PreviewDoc.aspx?saleItemID=40729 (accessed on 18 April 2016).
33. Che Haron, C.H. Investigation on the influence of machining parameters when machining tool steel using EDM. *J. Mater. Process. Tech.* **2001**, *1*, 84–87. [CrossRef]
34. Yan, B.H.; Tsai, H.C.; Huang, F.Y. The effect in EDM of a dielectric of a urea solution in water on modifying the surface of titanium. *Int. J. Mach. Tool Manuf.* **2005**, *2*, 194–200. [CrossRef]
35. Mižáková, J.; Hošovský, A.; Piteľ, J. Modeling of heat transfer through the wall for simulation of heating process control. In *Trudy IX Meždunarodnoj Naučno-Techničeskoj Konferencii*; Donskoj gosudarstvennij techničeskij universitet: Rostov Na Donu, Russia, 2010; pp. 298–301.
36. Saha, S.K.; Chaudhary, S.K. Experimental investigation and empirical modeling of the dry electrical discharge machining process. *Int. J. Mach. Tools Manuf.* **2009**, *49*, 297–308. [CrossRef]
37. Straka, L'.; Čorný, I. Mathematical model of influence of cutting current on machined surface roughness at electro-erosion cutting. In *Operation and Diagnostics of Machines and Production Systems Operational States*; Scientific Papers; Lüdenscheid: RAM-Verlag, Germany, 2009; pp. 71–77.
38. Mahapatra, S.S.; Patnaik, A. Optimization of wire electrical discharge machining (WEDM) process parameters using Taguchi method. *Int. J. Adv. Manuf. Technol.* **2007**, *34*, 911–925. [CrossRef]